NIPPON STEEL TECHNICAL REPORT No. 94 July 2006

UDC 622 . 341 . 1

Marra Mamba Ore, Its Mineralogical Properties and Evaluation for Utilization

Jun OKAZAKI*1 Kenichi HIGUCHI*1
Masanori NAKANO*1

Abstract

New Marra Mamba ore is expected to be another principal Australian iron ore following pisolite ore, and for this reason, establishing technology for its effective use is an important task for the people related to sintering. This paper reports the results of studies into its mineralogical properties and comparative evaluation of its granulating and melting properties with those of conventionally supplied ores. Technologies for increasing the use of the Marra Mamba ore based on the study results are also discussed.

1. Introduction

As the low-P Brockman ore came to be depleted, Marra Mamba ore, which has a high content of combined water (CW), was developed[1] as a substitute brand of Australian iron ore. The West Angelas ore was first shipped in 2002, and the ore (MAC ore) from Mining Area C in 2003, not blended with other brands[2]. The Marra Mamba ore has been mixed in the presently imported low-P Brockman ore since some time ago[2], and this indicates that the CW content of Australian ores will increase rapidly not only with the pisolite ores, the principal brand of Australian ore at present, but also with the increasing Marra Mamba ore. Of the Australian iron ores, the Marra Mamba ore is the second most abundant brand following the pisolite ore, and for this reason, establishing the technology for its effective use is an important task of the people related to sintering.

While some papers have reported the basic properties of the Marra Mamba ore[3-9], in consideration of further increase in its supply and of its use together with the pisolite ore, it is essential to fully understand its mineralogical properties.

This paper reports the results of our examination of the mineralogical properties of the Marra Mamba ore and reevaluates it based on the examination results.

2. Evaluation of Mineralogical Properties of Iron Ores

2.1 Ore specimens

The specimen of the Marra Mamba ore was called Ore W[3,4] for our tests. The following brands of ore were used as comparative specimens: two brands of Brazilian hematite ore (Ores A and B), two brands of Australian low-P hematite ore (Ores C and D), two brands of Australian pisolite ore, one containing high Al_2O_3 (Ore E) and the other low Al_2O_3 (Ore F), and Indian high-goethite ore (Ore G). A drum sample (350 kg) of each specimen ore was dried and then sieved to prescribed sizes.

2.2 Method of evaluation

2.2.1 Basic properties

2.2.1.1 Grain size distribution

Because the rate of fines significantly influences the granulability of ore, the percentage of fines 0.125 mm or less in size of each specimen was measured.

2.2.1.2 Chemical composition

Chemical composition of grains 2.0 to 2.8 mm in size, which serve as the cores of pseudo-particles, and that of grains 0.5 mm or less in size, which adhere to the cores to form pseudo-particles, were examined for each specimen. The components analyzed were T.Fe (the main component), SiO_2, Al_2O_3, and CW. Here, the CW content was determined by Karl Fischer method[10].

2.2.1.3 Mineralogical structure

Ore grains 2.0 to 2.8 mm in size were observed under an optic microscope. The ore grains were classified into the following four types according to the composition of the iron oxide constituting the ores: (1) all hematite, (2) mainly hematite with goethite making up the balance, (3) mainly goethite with hematite making up the bal-

*1 Environment & Process Technology Center

(Originally published in ISIJ. International, Vol. 45 (2005), No. 4, pp.427-435)

ance, and (4) all goethite. The number of the ore grains observed was approximately 120.

2.2.1.4 Volume and diameter distribution of pores

The volume and diameter distribution of the pores 200 μ m or less in diameter in ore grains 2.0 to 2.8 mm in size were measured using a mercury penetration porosimeter. The grains in the above size range were selected because they accounted for the largest part of sinter feed, and were most likely to serve as the cores of pseudo-particles.

2.2.1.5 Morphology of gangue minerals

Ore grains 2.0 mm or less in size were washed with water, and the samples of gangue minerals were collected from among the floating particles in the supernatant liquid. Using roughly 30 sample particles that looked to be gangue particles, the shape of the minerals was observed with a transmission electron microscope (TEM), and their chemical composition determined by energy dispersion X-ray spectroscopy (EDS).

2.2.2 Granulation ability

2.2.2.1 Cohesive strength of fine ores

The surface structure of coarse ore grains, which serve as the cores of pseudo-particles, is considered to have significant influence on the granulability of an ore brand[11,12]. However, once fines adhere to the surface of a coarse grain, the granulability of the fines presumably determines the grain growth thereafter. For this reason, the granulability was evaluated based on the cohesive strength of fines. The higher the cohesive strength of an ore brand measured by the method described below, the better we judged the granulability of the brand to be.

Samples were prepared by mixing ore grains of the following five size classes by 20 mass% each: 0.5 to 1.0 mm, 0.25 to 0.5 mm, 0.125 to 0.25 mm, 0.063 to 0.125 mm, and 0.063 mm or smaller. Then, changing the amount of water addition from 0 to 15 mass%, the cohesive strength was measured by the tensile breaking method[13].

2.2.2.2 Water absorption

The water absorption of the ores was measured by the centrifugal moisture equivalent method[14] using samples of ore grains 2.0 to 2.8 mm in size, which would serve as the cores of pseudo-particles, and those 1.0 mm or less in size, which would serve as the adhering fines. The grain size distribution of the grains 1.0 mm or less in size was the same as that in the measurement of the cohesive strength described above. The higher the value of an ore brand measured by the method, the more the brand was judged to absorb water. The result of this measurement gives an indication of the optimum moisture for granulation.

2.2.3 Melting characteristics

2.2.3.1 Melt penetration[15] (see **Fig. 1** (a))

Melt penetration tests were conducted using ore tablets simulating the adhered fine layer of a pseudo-particle and reagent tablets having a chemical composition of primary melt. The ore tablets (15 mm in diameter and 5 mm in height) were prepared by mixing ore grains of two size classes, namely 0.25 to 0.5 mm and 0.25 mm or smaller, by 50 mass% each, and pressing the mixture in a metal die at a pressure of 4 MPa. The composition of the reagent tablets was set at 26 mass% CaO + 74 mass% Fe_2O_3; this is close to the eutectic composition in the phase diagram of a CaO-Fe_2O_3 binary system proposed by Phillips et al[16]. The reagent tablets (5 mm in diameter and 5 mm in height) were prepared by mixing an Fe_2O_3 reagent and CaO reagent in a mortar for 20 min. and pressing the mixture in a metal die at a pressure of 4 MPa.

The test apparatus is shown schematically in Fig. 1. A reagent tablet was placed at the center of the upper surface of an ore tablet to form a sample set, the sample set was placed in a nickel crucible (20 mm in diameter and 15 mm in height), and heated in an electric furnace in a normal atmosphere. To simulate the operation of a commercial sintering machine, the sample sets were heated from 1100 to 1,290℃ in 1 min, cooled from 1,290 to 1,100℃ in 3 min, and when the temperature fell to 1,100℃, extracted from the furnace to cool down in the normal atmosphere. The sample sets were cut vertically along the centerline, the cut surface was polished, and the depth to which the primary melt penetrated was measured at the surfaces.

2.2.3.2 Assimilation with CaO (see Fig. 1 (b))

To evaluate the assimilation behavior of the ores with CaO, micro packed bed heating tests[17] were conducted using model pseudo-particles composed of each of the specimen ores and limestone. The pseudo-particles were prepared by coating ore grains 2.0 to 2.8 mm in size with limestone 0.5 mm or less in size using water. The mass

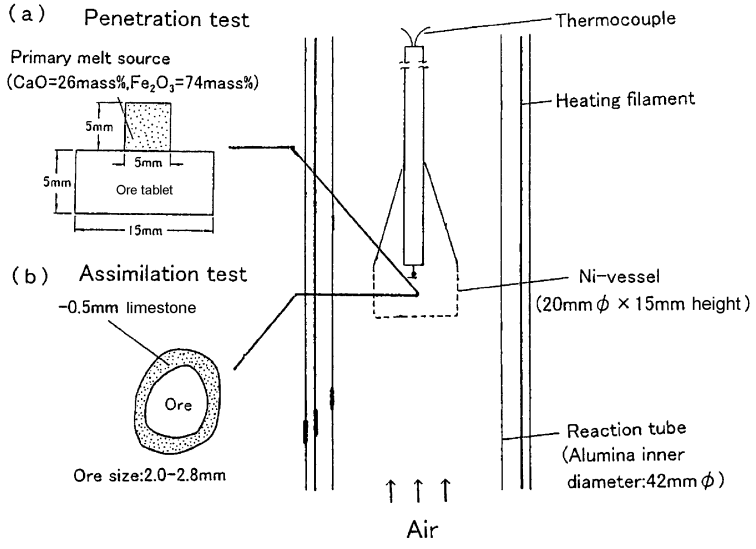

Fig. 1 Schematic diagram of experimental apparatus

ratio of CaO to ore (CaO/Ore) of the pseudo-particles was set at 0.1 simulating the feedstock mixture of a commercial sintering machine. The pseudo-particles thus prepared were put into a nickel crucible of the same size as the above to fill its inside, and heated to 1,300℃ in an electric furnace in a normal atmosphere. To simulate the operation of a commercial sintering machine, the pseudo-particles were heated from 1,100 to 1,300℃ in 1 min, cooled from 1,300 to 1,100 ℃ for 3 min in an electric furnace shown in Fig. 1, and when the temperature fell to 1,100℃, they were extracted from the furnace to cool down in the normal atmosphere. The sintered cake thus obtained was cut at the position 5 mm above the bottom of the crucible, the cut surface was polished, and mineralogical structure was observed at the surface. In addition, the void fraction (ε) of the sintered cake was measured by image processing of the section surface in a magnification × 5 using the following equation:

$$\varepsilon = (1 - V1 / V0) \times 100\ (\%) \qquad (1)$$

where

ε is void fraction (area %);

V0 is the inner sectional area of the nickel crucible (cm^2); and

V1 is V0 less the sectional area of the sintered cake excluding that of pores (cm^2).

3. Evaluation Results and Discussion

3.1 Basic properties

3.1.1 Grain size distribution

Fig. 2 compares the ore specimens with respect to the mass fraction of fine grains 0.125 mm or less in size. The graph shows that Ore W is characterized by the large mass fraction of fines. The high CW content of the ore grains 0.5 mm or less in size of Ore W, as seen with **Fig. 3**, suggests that the fines of Ore W contain goethite in a high percentage.

3.1.2 Chemical composition

Fig. 3 shows the chemical compositions of the ore specimens in a breakdown into two grain-size groups, from 2.0 to 2.8 mm and 0.5 mm or smaller. The composition difference between the two grain-size groups of all the ore specimens was substantially the same except for Ore A. Ore W had a high CW content, but its T.Fe was substantially the same as those of Ores C and D. Furthermore, Ore W was characterized also by the content of gangue lower than those of Ores C, D, E and F (conventional Australian ores): its SiO_2 content was 2.5 mass% and Al_2O_3 content 1.6 mass%, approximately.

3.1.3 Mineralogical structure

Fig. 4 shows the photomicrographs of some ore specimens. Ore C exhibited an aggregate structure composed of hematite (micro platy hematite) approximately 20 μ m in size, and so did Ore D (see Fig. 4 (c)). On the other hand, Ore W exhibited a structure in which grains of martite (hematite having a shape of a crystal of magnetite) roughly 50 to 100 μ m in size were mixed in fine goethite (see Fig. 4 (a)), and the martite grains were characterized by very smooth surfaces.

Fig. 5 compares Ore W with Ores C and D in terms of the composition of the types of iron oxide in the ore grains. Whereas grains mainly composed of hematite accounted for approximately 60% in Ores C and D, those composed entirely of goethite and those composed of goethite mixed with martite accounted for approximately 60% in Ore W. This difference in mineralogy of iron oxide phase between Australian ores was reported to be ascribed a difference in supergene enrichment process after BIF (Banded Iron Formation)[1].

3.1.4 Volume and diameter distribution of pores

Fig. 6 compares the ore specimens in terms of the volume of

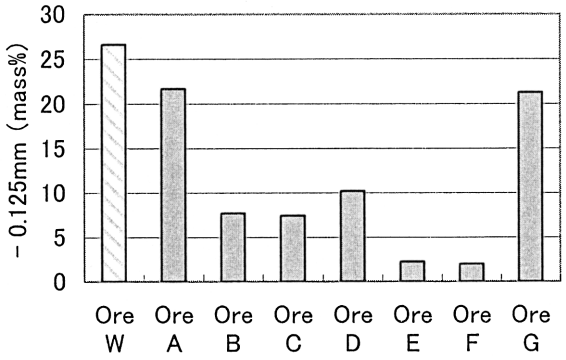

Fig. 2 Comparison of mass fraction of –0.125 mm in each ore

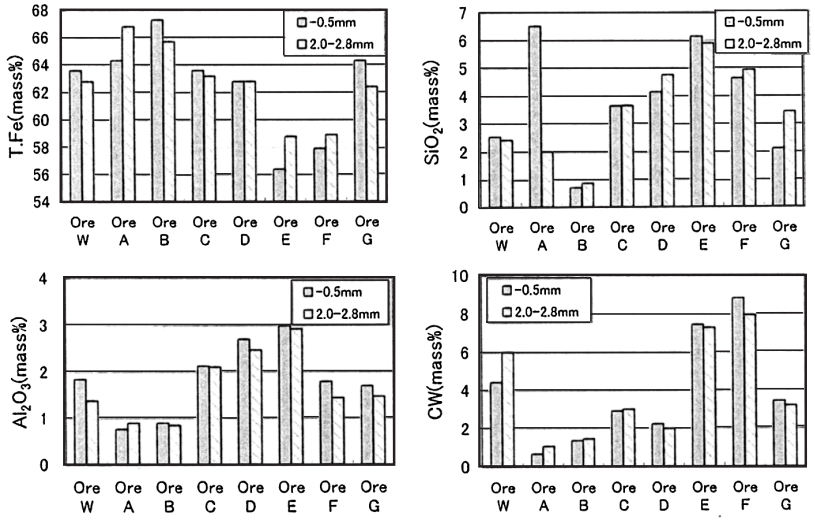

Fig. 3 Chemical compositions of coarse ores (2.0 - 2.8 mm) and fine ores (–0.5 mm)

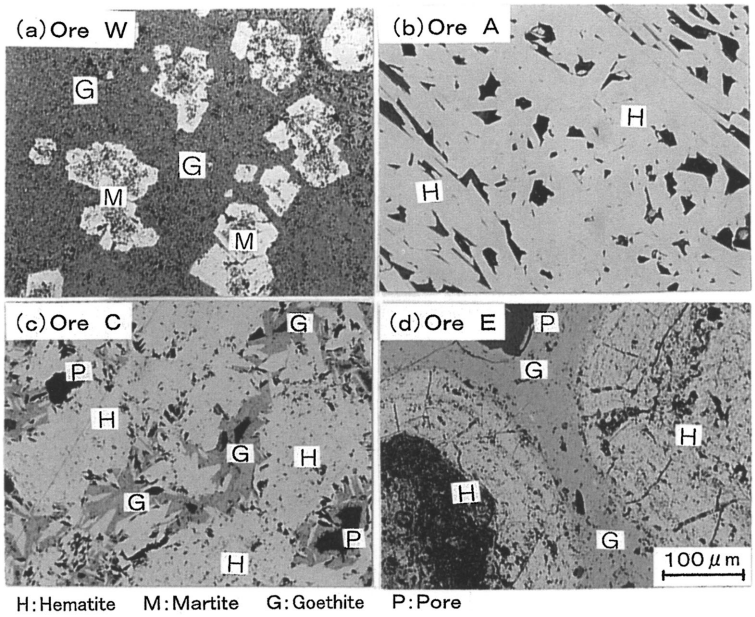

Fig. 4 Microstructure of ores before heating

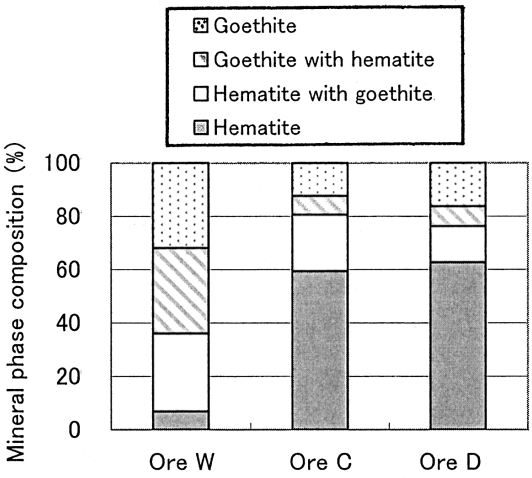

Fig. 5 Comparison of type distribution of iron oxide of coarse ores (2.0 - 2.8 mm). Hematite grains of Ore W exhibited martite structure

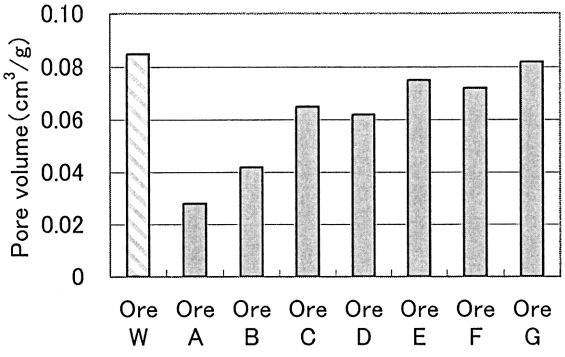

Fig. 6 Comparison of porosity of coarse ores (2.0 - 2.8 mm)

pores 200 μm or less in diameter. The pore volume of Ore W was 0.084 cm^3/g, higher than those of Ores C and D, and nearly the same as those of the high-porosity ores, namely Ore E, Ore F and Ore G.

Whereas the pore diameters of Ore W ranged mainly from 0.01 to 10 μm, those of Ores E and F were in a narrower range, mainly from 0.01 to 0.05 μm, and those of Ores C and D and Ore G in a wider range from 0.01 to 100 μm. This is presumably due to the difference in the mass fractions of the component iron oxides between these ores as shown in Fig. 5.

3.1.5 Morphology of gangue minerals

The TEM observation revealed stick-like and hexagonal tabular crystals in the gangue of Ore W (see **Fig. 7**); the former accounted for 70% of the total and the latter 30%, approximately. From their shape and EDS analysis, the latter was supposed to be kaolinite. Note that the hexagonal tabular crystals accounted for most of the gangue of Ore C[18].

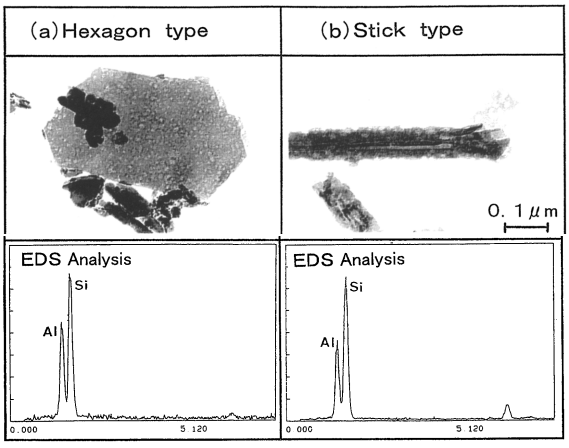

Fig. 7 Morphology and chemical composition of gangue minerals of Ore W (TEM image)

3.2 Granulation ability

3.2.1 Cohesive strength of fine ores

Fig. 8 shows the measurement results of the cohesive strength of fine ores. Whereas Ores C, D, E and F (conventionally supplied Australian ores other than the Marra Mamba ore) exhibited the largest cohesive strength with a moisture content of 5 to 6 mass%, the cohesive strength of Ore W was highest, roughly 13 g/cm^2, with a moisture of 10 mass%. This strength value was lower than those of the conventionally supplied Australian ores, and close to the cohesive strength of Brazilian ores of poor granulability.

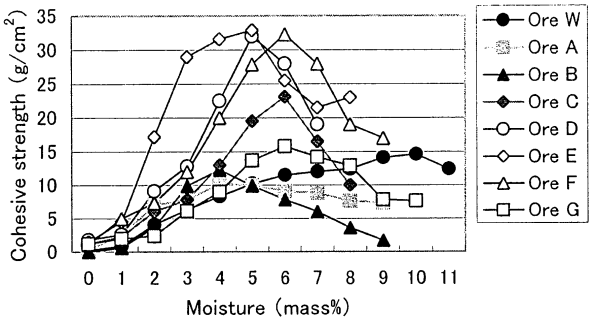

Fig. 8 Cohesive strength of fine ores (–1mm) for various moisture content

3.2.2 Water absorption

Fig. 9 shows the measurement results of the water absorption of the specimens. In either of the two grain-size ranges, Ore W exhibited higher water absorption than those of the other ore specimens. Especially in the grain size range of 1 mm or less, its water absorption was nearly twice those of Ores C, D, E and F (conventionally supplied Australian ores).

3.3 Melting characteristics

3.3.1 Melt penetration

Melt penetration depth is used in the commercial operation of sintering machines as an indicator for the control of sinter strength and yield[15]: the higher the value, the better the strength and yield. **Fig. 10** shows the measurement results of the melt penetration depths of the specimens. Whereas the melt penetration depths of Ores C, D, E and F (conventionally supplied Australian ores) were around 1.3 mm, that of Ore W was as large as 3.0 mm. A reason for this is

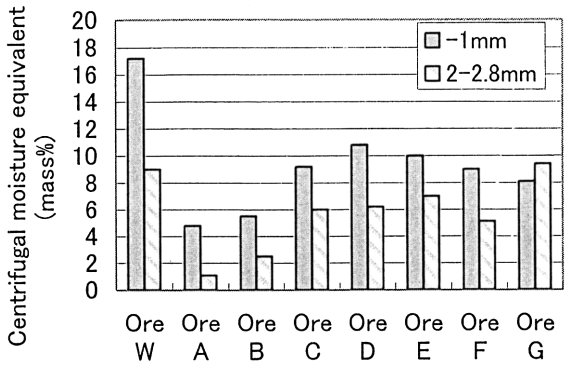

Fig. 9 Comparison of centrifugal moisture equivalent of coarse ores (2.0 - 2.8 mm) and fine ores (–1mm) by ore kind

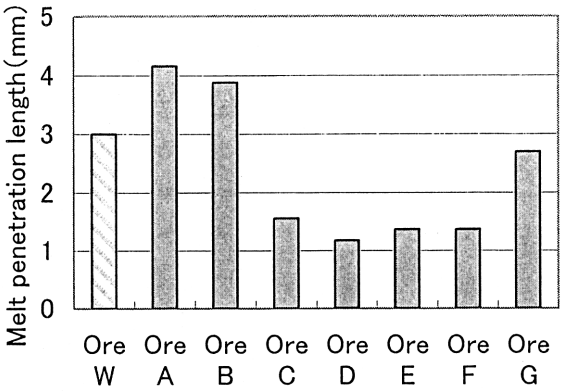

Fig. 10 Measurement results of melt penetration length of melt from fine ores

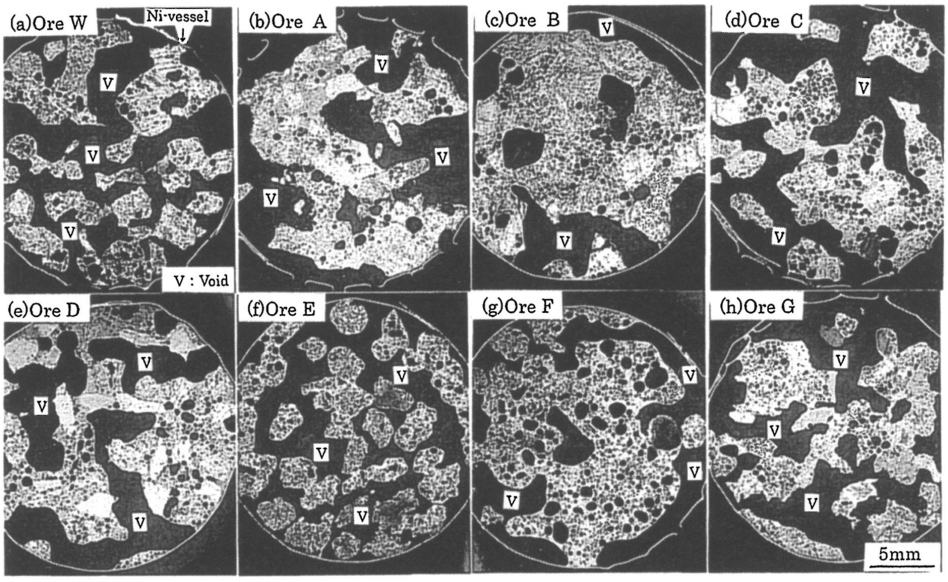

Fig. 11 Macro images of sintered ores after assimilation tests

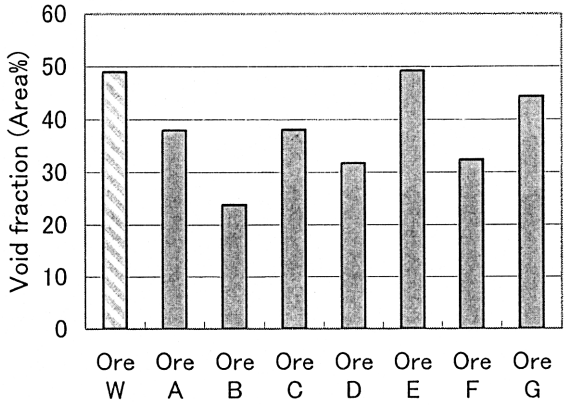

Fig. 12 Measurement results of void fraction of sinter after assimilation tests

presumably its smaller content of gangue compared with those of the other Australian ores. In relation to this, it was previously found and reported that the melt penetration depth tended to decrease with increasing contents of SiO_2 and Al_2O_3[15].

3.3.2 Assimilation with CaO

Fig. 11 shows the sectional macrostructures of the ore specimens after the assimilation test. The structure of Ore W was similar to that of Ore E. Many pores (voids) were observed in the sintered specimen, and for this reason, the strength was suspected to be low. **Fig. 12** shows the void fraction of the sintered specimen of the ore. The void fraction of Ore W was approximately 50%, higher than those of the other specimens. A high assimilation with CaO of coarse ore grains is considered a factor for lowering the strength and yield of sinter.

4. Evaluation of Mineralogical Properties of Marra Mamba Ore

4.1 Granulation ability

To improve the granulability of the Marra Mamba ore, it is necessary to increase its cohesion strength. High moisture granulation is an effective way to improve granulability, but as seen with Fig. 8, the cohesion strength of the Marra Mamba ore does not improve much with higher moisture. Presumably, a reason for this is that, as seen with Fig. 7, the ore contains only a small mount of gangue (kaolinite), which contributes to the improvement in granulability. Another reason is probably that, through the SEM observation, many pores 20 to 30 μm in diameter were found at the surfaces of Ore W (see **Fig. 13** (a)). This indicates that water is likely to go to the inside of ore grains through the pores, which means that it is difficult for water, which improves granulability, to stay on the grain surfaces. Therefore, to improve the granulability of the Marra Mamba ore, it was considered to be important to apply a pre-granulation process as explained later.

4.2 Melting properties

To improve the melting properties of the Marra Mamba ore, it is necessary to improve the assimilation properties of its coarse grains, which serve as the cores of pseudo-particles, because the ore does not form melt in a quantity sufficient for the adhesion of fines at a heating temperature of approximately 1,300℃. This is presumably due to the assimilation behavior described below.

At the microscopic observation of the assimilated portions of Ore W, calcium ferrite was found at the center portions of ore grains (see **Fig. 14** (a and b)); it was suspected that, owing to the high porosity of the brand, melt of a calcium ferrite system that formed through assimilation reactions penetrated to the inside of a grain through the pores.

On the other hand, ore grains having high contents of SiO_2 little assimilated with CaO and their surfaces were covered with melt of silicate (see Fig. 14 (c and d)). This is presumably because SiO_2 in the ore grains dissolved in the melt of a calcium ferrite system that formed on the grain surfaces, transforming the melt into silicate slag having a high melting temperature[19].

With respect to the melt penetration properties of fines, which adhere to the coarse grains to form pseudo-particles, on the other hand, the Marra Mamba ore was found superior to the conventionally supplied Australian ores; this seems to indicate that the fines of the Marra Mamba ore are effective in improving the sinter strength

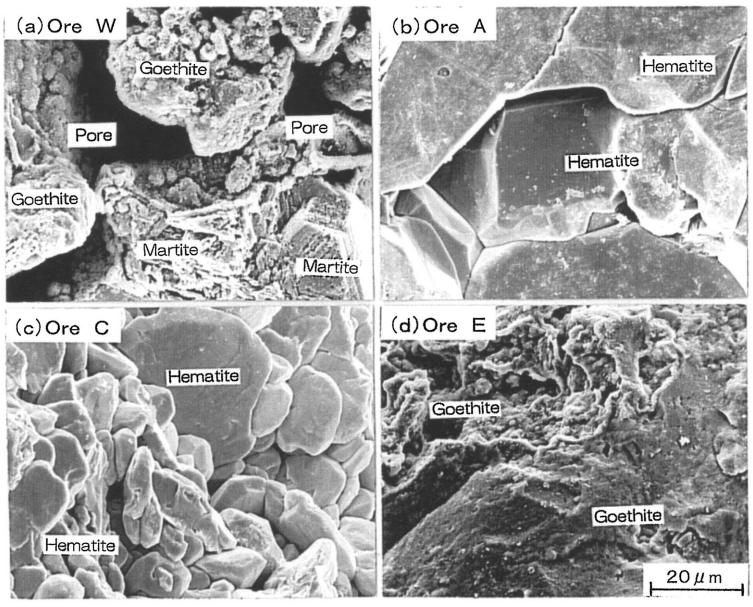

Fig. 13 SEM images of ore surfaces

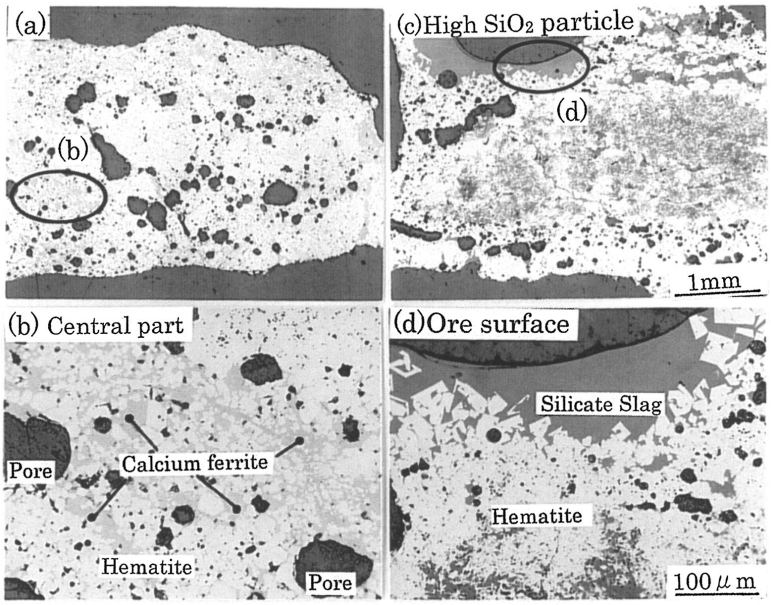

Fig. 14 Microstructures of sinter using Ore W after assimilation test. Magnification is × 20 for (a) and (c), × 200 for (b) and (d)

and yield.

As stated above, the melting properties the coarse grains, which serve as the cores of pseudo-particles, and those of the fines, which adhere to the coarse grains to form pseudo-particles, of the Marra Mamba ore were found to be quite different from each other. To increase the use of this ore brand, therefore, structural design of pseudo-particles in consideration of such characteristics is essential.

5. Discussion on Sintering Properties of Marra Mamba Ore

The problems in the sintering of the Marra Mamba ore were examined in consideration of the results of pot tests conducted by BHP-Billiton[20]. BHP-Billiton used the MAC ore for the tests; this brand has mineralogical properties similar to those of Ore W of our tests.

Fig. 15 shows the results of the pot tests of BHP-Billiton. A comparison between Blends 1 and 2 shows that, when 30% of the Mt. Newman ore (same as Ore D, Australian low-P, of our tests) was replaced with the MAC ore, while maintaining moisture substantially unchanged, the tumbler index of the product fell and the unit consumption of coke increased from those with 100% Mt. Newman ore. On the other hand, from a comparison between Blends 3 and 6, when the moisture was changed according to the amount of the MAC ore, the unit consumption of coke increased a little but the sinter strength was kept unchanged. The above indicates that, to increase the use of the Marra Mamba ore, it is necessary to increase the moisture of the mixture. This generally agrees with the results of our measurement of the cohesive strength described in sub-section 4.1 Granulation ability.

6. Technology for Increased Use of Marra Mamba Ore

The mini pellet process[21] commercially applied in 1987 at Fukuyama Works of JFE (then NKK) was a technology aiming at increasing the use of the Marra Mamba ore. This process is an increase in the mixing rate of the Marra Mamba ore to 10 mass% continuously at No. 4 Sintering Machine of the Works. The HPS process[22], which was applied to Fukuyama No. 5 Sintering Machine in 1988, made it possible to increase the mixing rate of the Marra Mamba ore further to 15 mass%. More recently, some papers reported that preliminary agitation of blended feedstock was effective in increasing the blending rate of the brand[23]. The selective granulation process[24] developed by Nippon Steel is also considered effective for the purpose. Besides these, the MEBOIS process[25] proposed by Kasai et al. is a revolutionary technology that makes it possible to increase the use of the Marra Mamba ore by pelletizing. All these technologies indicate that preliminary granulation treatment is essential for increasing the use of the ore brand.

7. Conclusion

The mineralogical properties of the new kind of Marra Mamba ore were investigated and the following findings were made.

(1) The Marra Mamba ore has a high content of CW, a high percentage of fines and a highly porous structure. On the other hand, its gangue amount is smaller than those of conventionally supplied Australian ore brands.

(2) The water absorption of the Marra Mamba ore is large owing to its high porosity, and as a result, its granulation requires higher moisture than in the cases of other ore brands. However, because of the small content of kaolinite, the gangue mineral, the cohesive strength of the brand does not improve much even with a high moisture.

(3) The melt penetration property of the fines, which adhere to the cores of pseudo-particles, of the Marra Mamba ore is good. Therefore, its use is considered effective in improving sinter strength and yield.

(4) Through assimilation with CaO, the coarse ore grains, which serve as the cores of pseudo-particles, of the Marra Mamba ore form a structure with a high void fraction. This is because, owing to the porous structure, the ore brand does not produce a sufficient amount of melt indispensable for bonding. On the other hand, the fines of the Marra Mamba ore exhibit excellent melt penetration, which is advantageous for improving sinter strength

Blend	Composition
1	Blend containing 100% Mt. Newman high grade fines; Basicity: 1.8; MgO: 1.5
2	Blend containing 70% Mt. Newman high grade fines, 30% MAC; Basicity: 1.8; MgO: 1.5
APB	Asia Pacific Blend (APB) containing ores from Australia, Brazil, India and Venezuela
3	Replacing 25% Mt. Newman high grade fines in APB with 20.8% Mt. Newman high grade fines and 4.2% MAC fines
4	Replacing 25% Mt. Newman high grade fines in APB with 16.7% Mt. Newman high grade fines and 8.3% MAC fines
5	Replacing 25% Mt. Newman high grade fines in APB with 25% MAC fines
6	Replacing 25% Mt. Newman high grade fines in APB with 13.4% Mt. Newman high grade fines and 8.3% MAC, 3.3% OB29

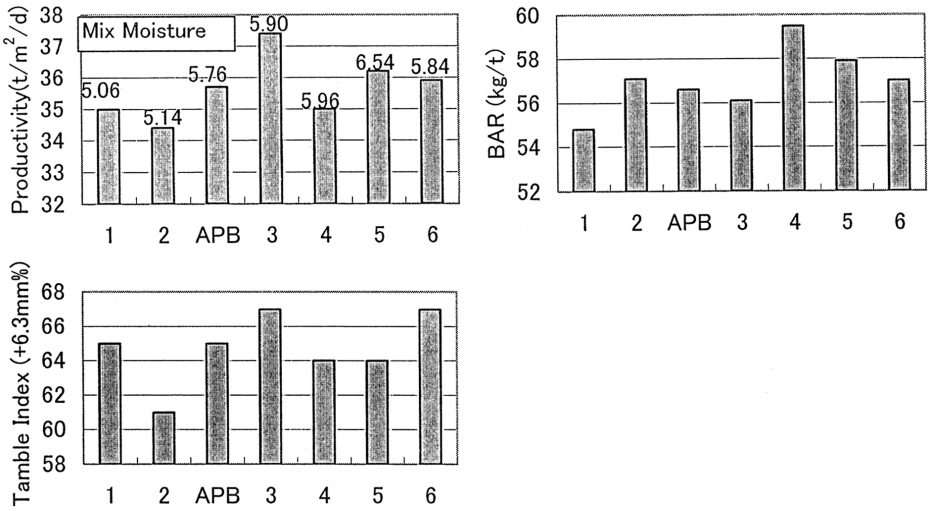

Fig. 15 Pot test results for evaluation of the influence of Marra Mamba ores (MAC) on sintering performance conducted by BHP Billion[20)]

and yield.

(5) Pretreatment for intensive granulation is effective in increasing the mixing rate of the Marra Mamba ore; pelletizing is especially effective for the purpose.

References

1) Hida, Y., Nosaka, N.: Tetsu-to-Hagané. 78, 960(1992)
2) Nagano, K.: Tetsu-to-Hagané. 90, 51(2004)
3) Okazaki, J., Nakano, M., Hosotani, Y.: CAMP-ISIJ. 14, 187(2001)
4) Okazaki, J., Hosotani, Y.: CAMP-ISIJ. 14, 952(2001)
5) Loo, C.E., Bewsher, A., Hutchens, M.F.: CAMP-ISIJ. 12, 172(1999)
6) Hida, Y., Nosaka, N.: CAMP-ISIJ. 16, 52(2003)
7) Dukino, R., Ingland, B., Hutchens, M.F.: CAMP-ISIJ. 16, 173(2003)
8) Waters, A., Khosa, J.: CAMP-ISIJ. 17, 124(2004)
9) Clout, J., Manuel, J., Bergstr, R., Waters, A.: CAMP-ISIJ. 17, 125(2004)
10) JIS. M 8211
11) Katsuhiko, K.: Fusen. 28, 99(1981)
12) Maeda, T., Shimizu, M., Fukumoto, T.: CAMP-ISIJ. 16, 83(2003)
13) Rumpf, H., Schubert, H.: J. Chem. Eng. 7, 83(1974)
14) Haruna, J., Suzuki, S., Yamada, H.: Tetsu-to-Hagané. 70, 103(1984)
15) Okazaki, J., Higuchi, K., Hosotani, Y., Shinagawa, K.: ISIJ. Int. 43, 1384(2003)
16) Phillips, B., Muan, A.: J. Am. Ceram. Soc. 41(11), 488(1958)
17) Okazaki, J., Hida, Y.: CAMP-ISIJ. 2, 47(1989)
18) Okazaki, J., Hida, Y.: CAMP-ISIJ. 6, 898(1993)
19) Hida, Y., Okazaki, J., Ito, K., Hirakawa, S.: Tetsu-to-Hagané. 78, 1013(1992)
20) Loo, C.E., Bewsher, A., Hutchens, M.F.: CAMP-ISIJ. 12, 174(1999)
21) Nakajima, R., Komatsu, O., Shimizu, M., Inoue, H., Takagi, A.: Tetsu-to-Hagané. 73, 765(1987)
22) Niwa, Y., Sakamoto, N., Komatsu, O., Noda, H., Kumasaka, A.: ISIJ.Int. 33, 454(1993)
23) Matsumura, T., Okata, T., Yamagata, T.: CAMP-ISIJ. 16, 910(2003)
24) Haga, T., Oshio, A., Kasama, S.: Tetsu-to-Hagané. 83, 169(1997)
25) Kasai, E.: CAMP-ISIJ. 15, 718(2002)